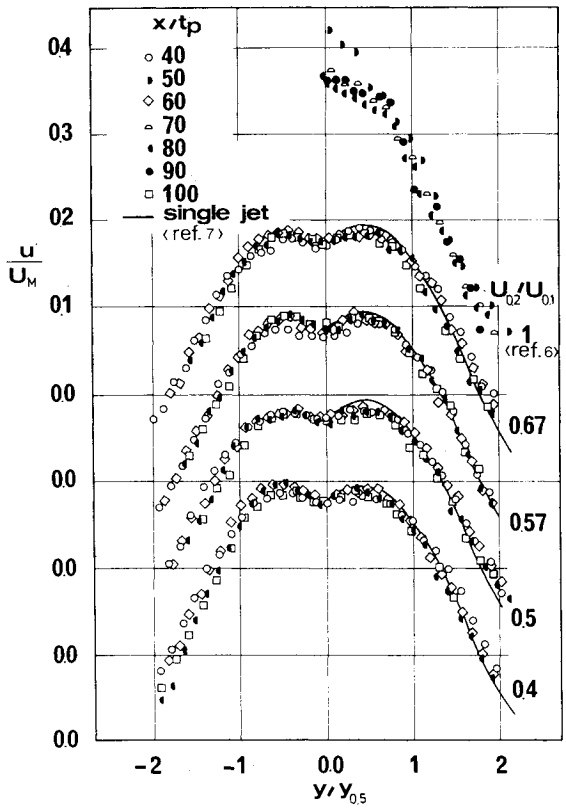

Fig. 3 Axial velocity fluctuations for combined intercepting jets.

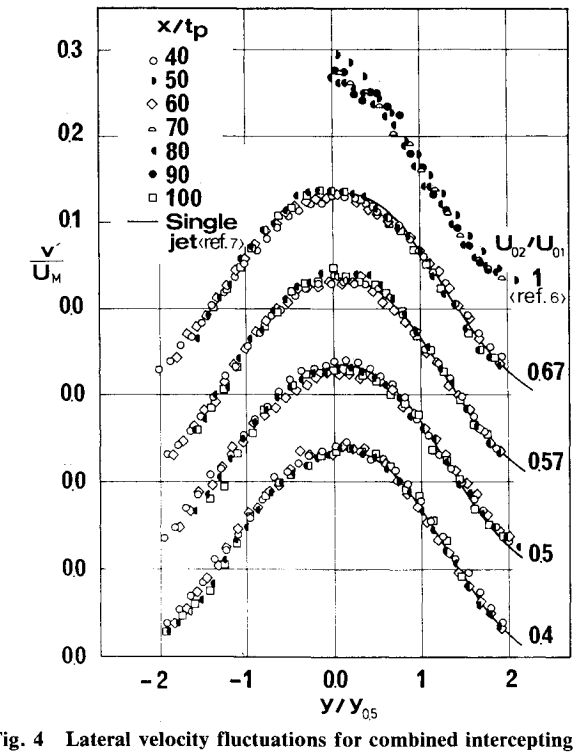

Fig. 4 Lateral velocity fluctuations for combined intercepting jets.

which would be obtained from simple momentum considerations if there were a zero net pressure force acting on the flowfield. Mutual entrainment of air by the two jets creates low pressure upstream of the merging region, which provides a transverse force tending to increase the deflection angle. However, due to confluence, high pressure is developed in and near the confluence region,[7] which results in an adverse effect on the deflection angle. The present results show a slightly smaller deflection angle as a net effect of the pressure field of the two merging jets. In the results of Foss[5] displayed in Fig. 1, positive pressure is developed in the pocket bounded by the two jets and the setback and standoff walls, resulting in a decreased deflection angle.

The growth of the half-width of the velocity in the combined jet is found to be linear with x, but with slightly lower rate than that for the single jet. The mean velocity profiles are shown in Fig. 2. The profiles are similar and agree well with that of a single jet.

The distribution of the axial velocity fluctuations u' are shown in Fig. 3. The plots show that the u' profiles are similar in the range of $x/t_p = 40 \sim 100$ and are close to the u' profile of the single jet. Figure 4 indicates that the lateral velocity fluctuations v' also have similar profiles in agreement with the v' profiles for the single jet.

Acknowledgments

The financial support was provided under a research project on Oil Well Fire Fighting (OWFF) sponsored by the Ministry of Petroleum and Minerals of Saudi Arabia.

References

[1]Murai, K., Taga, M., and Akagaw, K., "An Experimental Study on Confluence of Two Two-Dimensional Jets," *Bulletin of the JSME*, Vol. 19, No. 134, 1976, pp. 958-964.

[2]Krothapalli, A., Baganoff, D., and Karamcheti, K., "Development and Structure of a Rectangular Jet in a Multiple Jet Configuration," *AIAA Journal*, Vol. 18, Aug. 1980, pp. 645-650.

[3]Krothapalli, A., Baganoff, D., and Karamcheti, K., "Partially Confined Multiple Jet Mixing," *AIAA Journal*, Vol. 19, March 1981, pp. 324-328.

[4]Raghunathan, S. and Reid, I. M., "A Study of Multiple Jets," *AIAA Journal*, Vol. 19, Jan. 1981, pp. 124-127.

[5]Foss, J. F., "Flow Characteristics of the Defined Region Geometry for High-Gain Proportional Amplifiers," *Proceedings of 1967 Fluidics Symposium*, The American Society of Mechanical Engineers, Chicago, May 1967, pp. 45-61.

[6]Ram, C. S. and Kar, S., "Studies on Plane Interacting Jets," Paper presented at 10th SICE Fluidic Symposium, Tokyo, Oct. 1975.

[7]Elbanna, H., Sabbagh, J., and Rashed, M. I. I., "Interception of Two Equal Turbulent Jets," *AIAA Journal*, Vol. 23, July 1985, pp. 985-986.

[8]Elbanna, H., Gahin, S., and Rashed, M. I. I., "Investigation of Two Plane Parallel Jets," *AIAA Journal*, Vol. 21, July 1983, pp. 986-991.

Inlet Vortex Formation due to Ambient Vorticity Intensification

H.W. Shin,* W.K. Cheng,† E.M. Greitzer,‡ and C.S. Tan§
Massachusetts Institute of Technology
Cambridge, Massachusetts

INLET operation near the ground is often associated with the presence of a strong vortex stretching between the ground and the inlet face. Investigations of this "inlet vortex" (or ground vortex) have identified two basic mechanisms

Received Jan. 4, 1985; revision received April 26, 1985.

*Postdoctoral Associate, Department of Aeronautics and Astronautics (presently with General Electric Co., Cincinnati, OH). Member AIAA.

†Associate Professor, Department of Mechanical Engineering. Member AIAA.

‡Professor, Director, Gas Turbine Laboratory, Department of Aeronautics and Astronautics. Associate Fellow AIAA.

§Research Associate, Department of Aeronautics and Astronautics.

responsible for its formation.[1] This Note describes an experimental study of one of these, amplification of the component of ambient vorticity perpendicular to the ground as the vortex lines are convected into the inlet.

Experimental Setup

The experiments were designed to simulate an aircraft engine in near-static operation in proximity to a ground plane. They were conducted in the MIT Wright Brothers Wind Tunnel, which is a closed circuit with an elliptical test section 3.05 m wide, 2.3 m high, and 4.6 m long. In the experiments, a ground plane was mounted 0.5 m above the bottom of the test section.

The inlet model was a circular cylinder with no centerbody. Inside and outside diameters were 0.15 and 0.2 m, respectively. The tests were run with the inlet facing upstream, with an average Mach number in the inlet throat area of approximately 0.3. A layout of the experiment is shown in Fig. 1, which also indicates the upstream velocity profile and the ambient vorticity direction. Details of the configuration are given in Ref. 2.

Velocity and stagnation pressure measurements were made in the inlet with a 45 deg slanted hot wire and a Kiel probe, respectively. Traversing the hot wire across the inlet along a diameter, plus rotating the inlet, allowed measurement locations over the whole inlet face. At each location on the face, the hot wire was positioned at three probe angle orientations to resolve the three velocity components.[3-5]

The upstream shear flow used is shown in Fig. 2. The nondimensional velocity U/U_{ref}, where U_{ref} is the velocity at tunnel midwidth, is plotted vs the nondimensional distance across the tunnel. The measurement station corresponds to the inlet lip plane. Various symbols denote data taken at different heights above the floor, with U_{ref} of 4 m/s. The heights were selected so that alternate measurement stations were directly behind the strips and the open areas of the nonuniform grid used for shear generation. Except for the top position (which is expected to be outside of the capture area), sufficient mixing on a strip-to-strip scale occurred so that the variations in velocity due to individual wakes were small.

Experimental Results

The dashed curve in Fig. 2 has been fitted through the average of the measurements and the velocity profile can be seen to be approximately linear over the center 1.2 D of the tunnel. As shown in Fig. 1, this velocity profile represents a vertical (i.e., perpendicular to the ground plane) component of the ambient vorticity, which is essentially constant over the captured stream tube area (outside of the ground boundary layer). The nondimensional value of this ambient vorticity ω_∞ was $\omega_\infty D/U_c = 0.11$, where D is the inlet outer diameter and $U_c (= 1.15 U_{ref})$ the velocity at the location of the inlet centerline, as is indicated in Fig. 2. The vorticity is calculated using the overall velocity difference; this corresponds to a value of ω_∞ of 2.6 s^{-1}.

The measurements were carried out at conditions of $H/D = 1.13$, $U_{inlet}/U_c = 22$, where H is the inlet centerline height and U_{inlet} the average inlet velocity. In the tests, the inlet was placed far enough behind the grid so that the upstream potential field of the inlet did not affect the flow through the grid.

At low H/D and/or high U_{inlet}/U_c, a strong vortex was formed. The sense of the vortex was, as discussed in Ref. 1, in accord with the conceptual picture of (vertical) vortex lines entering the lower part of the inlet (see the photographs in Ref. 1). As a check on the causal relationship between the shear flow and the vortex formation, the grid was reversed (side-to-side) in the tunnel so that regions of high and low velocity were reversed. When this was done, the sense of the inlet vortex rotation was also reversed.

The stagnation pressure map in the inlet is presented in Fig. 3. (These and the velocity measurements were made at a station 1.4 D from the inlet lip.) Over most of the inlet face, the contours show the results of a roughly symmetric (left-right) ingestion of the linear far upstream velocity profile, with the

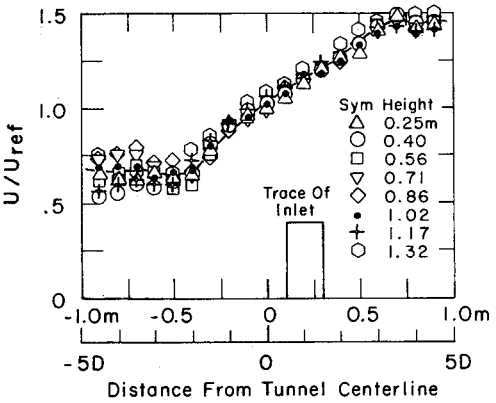

Fig. 2 Shear flow velocity profile across tunnel.

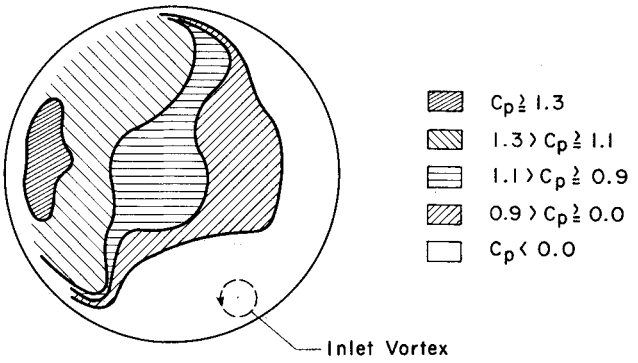

Fig. 3 Stagnation pressure contours in inlet: $C_p = (P_t - P_{sref})/(P_t - P_s)_{ref}$ (ref: pitot tube in middle of test section).

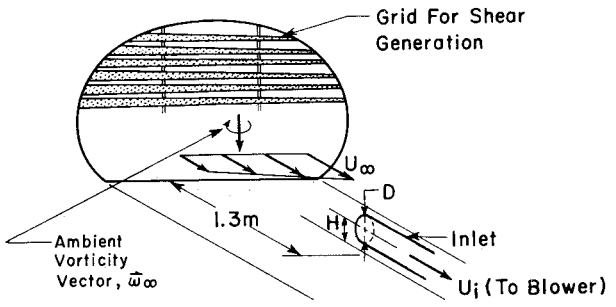

Fig. 1 Experimental configuration.

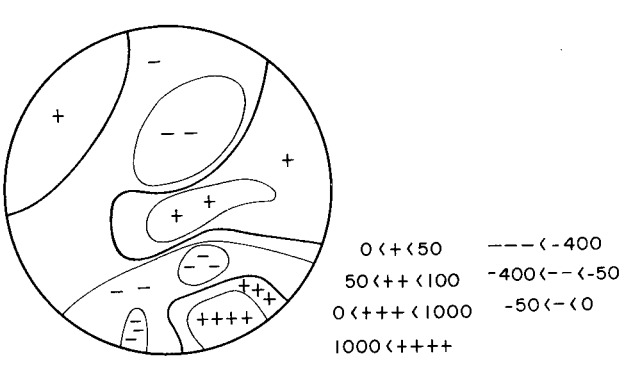

Fig. 4 Axial component of vorticity in inlet.

isobars close to vertical. However, there is a clockwise skewing of these isobars, which is consistent with a weak induced circulatory motion at the upper half of the inlet. This was implied in the vorticity distributions given by the calculations, as in Figs. 7-11 of Ref. 1.

In the lower part of the inlet, there is a substantial region of lower stagnation pressure. This ocurs in the neighborhood of the inlet vortex. The cross-plane velocities in this region are also considerably higher, the measurements showing values up to almost half the streamwise velocities. The position of the inlet vortex core is offset about 25 deg from the vertical (i.e., is at roughly "five o'clock"). This shift is associated with the induced velocity field of the inlet vortex in the presence of solid boundaries.

A map of the axial component of vorticity in the inlet, computed from the measured velocity, is shown in Fig. 4. Contours of ω_x/ω_∞, the local axial vorticity nondimensionalized by the upstream value, are plotted in the figure. Note that obtaining the vorticity involves, in some regions, the difference of two large velocities. In addition, for this flow, the vorticity is not a monotonically varying quantity, but rather varies strongly over the face. Thus, although the central features shown in Fig. 4 are unambiguous, some of the details should be viewed with this in mind.

Several features are apparent. First, as expected, the inlet vortex is a region of high vorticity due to vortex stretching. Also, because the vorticity varies so strongly over the face, the assigning of "a" circulation to the inlet vortex is somewhat arbitrary. However, we have computed the circulation around various contours to obtain several measures of this quantity and, based on these results, a reasonable value of the inlet vortex circulation for the present configuration (i.e., specified H/D, U_i/U_c), normalized by the upstream vorticity and capture area cross section, A_∞ ($A_\infty = U_i A_i/U_c$, where A_i is the inlet area), is

$$\frac{\Gamma}{\omega_\infty A_\infty} = \frac{\Gamma}{\omega_\infty U_i A_i/U_c} \simeq 2$$

As far as the authors are aware, this is the first time a measurement of this quantity has been made.

A second feature is a region of high vorticity of the opposite sign (from that associated with the inlet vortex) above and to the left of the inlet vortex. This marks the other leg of (or some of) the ingested vortex lines, the lower parts of which form the core of the inlet vortex. As shown in the calculations in Ref. 1, there should be substantial stretching of these opposite-sign vortex filaments in the region below the inlet centerline; this is seen in the data. What was not seen, however, is the large magnitude of this opposite-sign vorticity, as well as its nonsymmetric distribution—both of which are results of the mutual induction of the two opposite legs and the interaction with the solid boundaries. These effects, which are associated with the nonlinearity of the problem, are not included in the calculations.

The third feature is the weak circulation in the upper half of the inlet, again of the opposite sign from the inlet vortex as predicted by the calculations, although no real quantitative comparisons can be made because of the level of uncertainty in the data.

Summary and Conclusion

Measurements have been carried out to illustrate the nature of an inlet vortex in a flow with a vertical component of ambient vorticity. It is the amplification of this vorticity (by stretching) as the vortex lines are drawn into the inlet that is responsible for the vortex formation. Features of the amplification shown by the velocity measurements inside the inlet are a strong vortex, associated with the ground leg, at the lower part of the inlet at roughly "five o'clock" and, immediately above and to the left, a region of high vorticity of the opposite sign. The latter marks the other leg of the ingested vortex lines. The experiments show qualitative agreement with calculations based on a secondary flow approach,[1] although there are differences due to the nonlinear effects that occur in the actual phenomenon.

Acknowledgment

This work was sponsored by the Air Force Office of Scientific Research under Contract F49620-82-K-0002, Dr. J.D. Wilson, Program Manager.

References

[1]De Siervi, F., Viguier, H.C., Greitzer, E.M., and Tan, C.S., "Mechanisms of Inlet Vortex Formation," *Journal of Fluid Mechanics*, Vol. 124, 1982, pp. 173-207.

[2]Liu, W., "Design and Analysis of an Experimental Facility for Inlet Vortex Investigation," Gas Turbine Lab., Massachusetts Institute of Technology, Cambridge, Rept. 166, 1982.

[3]Whitfield, C.E., Kelley, J.C., and Barry, B., "A Three-Dimensional Analysis of Rotor Wakes," *Aeronautical Quarterly*, Vol. 23, Nov. 1972, pp. 285-300.

[4]Schmidt, D.P. and Okiishi, T.H., "Multistage Axial-Flow Turbomachine Wake Production, Transport and Interaction," *AIAA Journal*, Vol. 15, Aug. 1977, pp. 1138-1145.

[5]Shin, H.W. and Shippee, C., "Quantitative Investigation of Inlet Vortex Flow Field," Gas Turbine Lab., Massachusetts Institute of Technology, Rept. 179, March 1984.

Turbulent Boundary-Layer Wall Pressure Fluctuations Downstream of a Tandem LEBU

George B. Beeler*
NASA Langley Research Center, Hampton, Virginia

Nomenclature

C_f	= skin-friction coefficient = τ/q_∞
d^+	= effective transducer diameter scaled by wall units dU_τ/ν
h	= height of LEBU from splitter plate
p'_w	= rms wall pressure fluctuation
q_∞	= freestream dynamic pressure
U_∞	= freestream velocity
U_τ	= skin-friction velocity = $\sqrt{\tau/\rho}$
x	= streamwise coordinate
x_0	= location of δ_0 and first LEBU
δ_0	= initial turbulent boundary-layer thickness
δ^*	= displacement thickness
$\phi(\omega)$	= power spectral density of p'_w
τ	= wall shear stress
ρ	= density
ν	= kinematic viscosity
ω	= circular frequency

Introduction

TURBULENT wall pressure fluctuations (p'_w) are a source of noise and inaccuracy for passive SONAR.[1] The injection of polyethylene oxide or certain other polymers into the turbulent boundary layer reduces p'_w in water,[2] but requires

Received July 6, 1984; revision received July 22, 1985. This paper is declared a work of the U.S. Government and is not subject to copyright protection in the United States.

*Aerospace Engineer, Viscous Flow Branch, High-Speed Aerodynamic Division. Member AIAA.